



Power variations of Schumann resonances related to El Niño and La Niña phenomena

Heng Yang¹ and Victor P. Pasko¹

Received 20 March 2007; revised 20 March 2007; accepted 2 May 2007; published 2 June 2007.

[1] A three dimensional Finite Difference Time Domain (FDTD) model of the Earth-ionosphere cavity with the realistic conductivity profile is employed to study the intensity variations of Schumann resonances (SR) associated with the El Niño and La Niña phenomena. Comparison of the results derived from our FDTD model and the previous studies by other authors on related subjects shows that the intensity of the Schumann resonances varies with the spatial shifts of the thunderstorm regions under El Niño and La Niña conditions. Due to the different spatial field distributions of SR electrical and magnetic components in the Earth-ionosphere cavity, the different power variation patterns are clearly observed in the electrical and magnetic components with the motion of the thunderstorm center in our FDTD results. A new method is proposed to detect the shifts of the thunderstorm regions related to the El Niño and La Niña phenomena using the combination of both electrical and magnetic components of Schumann resonances at a single station. **Citation:** Yang, H., and V. P. Pasko (2007), Power variations of Schumann resonances related to El Niño and La Niña phenomena, *Geophys. Res. Lett.*, *34*, L11102, doi:10.1029/2007GL030092.

1. Introduction

[2] The highly conducting terrestrial surface boundary and the highly conducting ionospheric boundary separated by a weakly conducting atmosphere form a spherically concentric cavity, the Earth-ionosphere cavity, for the propagation of the electromagnetic waves produced by global lightning activity. Due to the conduction losses in the cavity, only electromagnetic signals below 100 Hz can propagate long distances without suffering serious attenuation, and the interference between the direct wave and the antipodal wave produces global resonances [Sentman, 1995; Nickolaenko and Hayakawa, 2002, pp. 158]. The resonance properties of the Earth-ionosphere cavity were first predicted and discussed by Schumann [1952], so these resonances are commonly referred to as Schumann Resonances (SR). Because the SR parameters (e.g., power, frequency, and Q-factor) are mainly determined by the global lightning activity and the electromagnetic properties of the lower ionosphere, observations of SR have been used in many applications to remotely sense the global lightning activity, the global climate variation, and the planetary scale variability of the lower ionosphere [e.g., Williams, 1992].

[3] The FDTD technique [e.g., Taflove and Hagness, 2000] represents one of the simplest and most flexible means for finding electromagnetic solutions in a medium with arbitrary inhomogeneities, and several reports about application of this technique to solution of VLF/ELF propagation problems in the Earth-ionosphere cavity have recently appeared in the literature [e.g., Pasko et al., 1998; Otsuyama et al., 2003; Simpson and Taflove, 2004; Yang and Pasko, 2005, 2006; Hu and Cummer, 2006; Yang et al., 2006].

[4] In our previous paper [Yang and Pasko, 2006], the diurnal and seasonal variations of SR parameters have been discussed in the context of a 3D FDTD model with an asymmetric conductivity profile. However, the positions of the simulated lightning sources are fixed in these simulations. In the present paper, the positions of the simulated sources are shifted southward and northward to account for the El Niño and La Niña phenomena, respectively. The associated SR power variations of the electrical and magnetic components derived from our FDTD model results are compared with previous experimental measurements by Satori and Zieger [1999]. We also present a new method to detect the spatial shifts of the thunderstorm regions using the combination of both electrical and magnetic components of Schumann resonances measured at a single station.

2. Model Formulation

[5] In present paper, a 3D FDTD model [Yang and Pasko, 2005] is employed to solve the ELF problems in the Earth-ionosphere cavity. The number of FDTD cells in θ and ϕ directions are 60 and 40, respectively. In r direction, the grid size is chosen to be 5 km. The time step Δt is determined by the Courant condition [e.g., Taflove and Hagness, 2000, pp. 136]. The cavity is excited by a vertical lightning current with 5 km length, which has a linear rise time 500 μ s and exponential fall with time scale 5 ms. The reported results for frequencies <40 Hz are not sensitive to the specifics of the chosen lightning current waveform. The power of each SR mode shown in present paper is derived from the maximum power appearing in the simulated spectrum.

[6] In the Earth-ionosphere cavity, the lightning activity mainly concentrates in three major areas: South-East Asia, Africa and South America. The magnitude of the lightning activity in these three regions reaches the peak at different time in the diurnal cycle [Sentman, 1995]. Figure 1a indicates the diurnal variation of the relative power of the global lightning activity in the three major lightning regions [Sentman and Fraser, 1991]. The total lightning activity in South-East Asia, Africa, and South America reaches maximum at approximately 0800, 1400, and 2200 UT, respectively. In our simulations, the peak power of the first SR

¹Communications and Space Sciences Laboratory, Pennsylvania State University, University Park, Pennsylvania, USA.

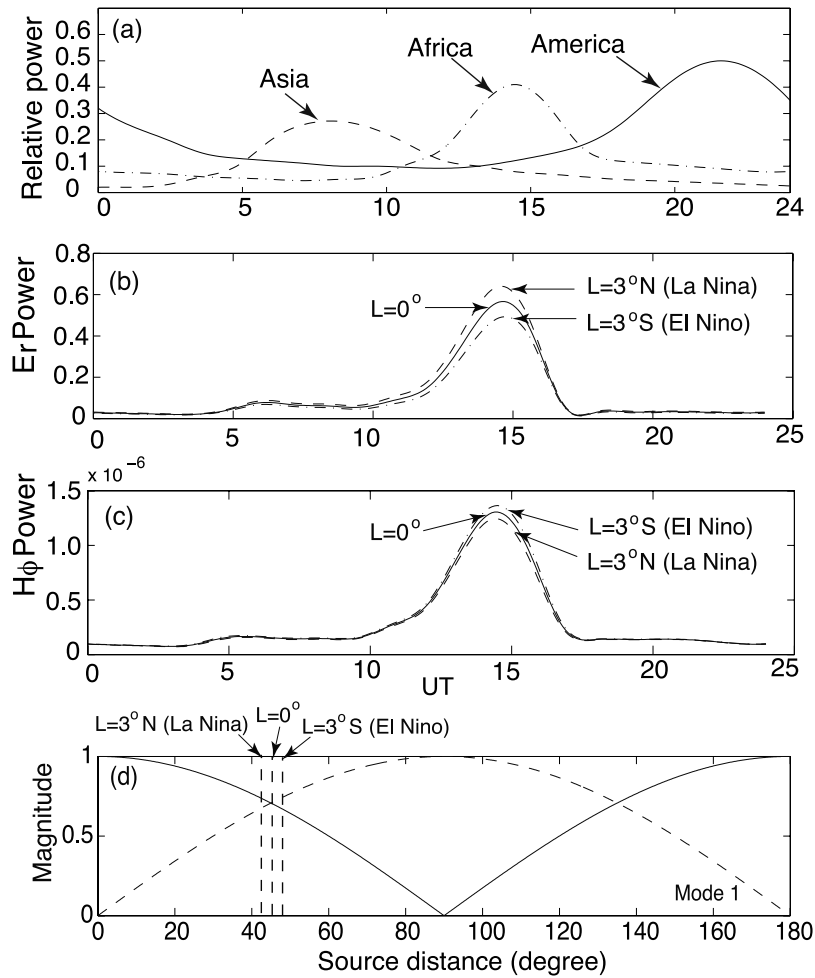


Figure 1. (a) The diurnal variation of the average lightning activity in the Southeast Asia, Africa, and America in September [Sentman and Fraser, 1991]. The diurnal power variations in (b) the E_r and (c) H_ϕ components of the first SR mode (L , the latitude of the lightning center in Africa). (d) The spatial distribution functions of the first SR mode in the Earth-ionosphere cavity (solid lines, E_r component; dashed lines, H_ϕ component).

mode is calculated every 1.2 hour from 0000 UT to 2400 UT. Three simulations are performed at each specific time point. In each simulation, the sources are activated in three regions centered at $27^\circ E$ $0^\circ S$, $99^\circ E$ $0^\circ S$, and $63^\circ W$ $0^\circ S$, corresponding to the three main lightning regions at Africa, South-East Asia and South America, respectively, in the case without El Niño and La Niña phenomena. The size of each source region is assumed to be $2000 \text{ km} \times 2000 \text{ km}$ with the lightning discharges uniformly distributed in this region [e.g., Yang and Pasko, 2006]. To account for the influence of the El Niño and La Niña phenomena on the global lightning activity, the simulated lightning source in Africa is moved 3° southward and northward in the simulations, respectively. A drift of the African thunderstorm region is estimated to be 4° – 8° in latitude between El Niño and La Niña years [Sátori and Zieger, 1999]. Nickolaenko and Hayakawa [2002, pp. 264] discussed related 10° shifts of African and American lightning centers. Therefore, the total 6° shift assumed in our simulations is reasonable for accounting for the movement of the lightning center in Africa related to El Niño and La Niña phenomena.

[7] The magnitude of each source at three major lightning regions was modulated as a function of time to reflect the

lightning activity variation shown in Figure 1a. Since the Earth-ionosphere cavity can be considered as a linear system, we can deal with these three sources separately. The total signal used in the final analysis can be expressed by the sum of the waves from these three sources. The modeling receiver is located at $\theta = 45^\circ$ and $\phi = 18^\circ$ just above the ground corresponding to the location of the SR field station ($47.6^\circ N$, $16.7^\circ E$) at Nagycenk, Hungary [Sátori and Zieger, 1999]. The vertical electrical field component (E_r) and magnetic component in east-west (H_ϕ) direction are calculated and compared with realistic measurements reported in [Sátori and Zieger, 1999; Price and Melnikov, 2004].

[8] The SR parameters are sensitive to the electromagnetic properties of the Earth-ionosphere cavity, which are mainly determined by the conductivity distribution in the cavity. In the present paper, the conductivity profiles are derived following the method we have reported in our previous work [Yang and Pasko, 2006]. At altitude $<60 \text{ km}$, the total conductivity is dominated by the ion conductivity, σ_i . The ion conductivity profile is taken from [Hale, 1984; Huang et al., 1999]. Above 60 km , the electron conductivity σ_e is dominant over the ion conductivity, and can be

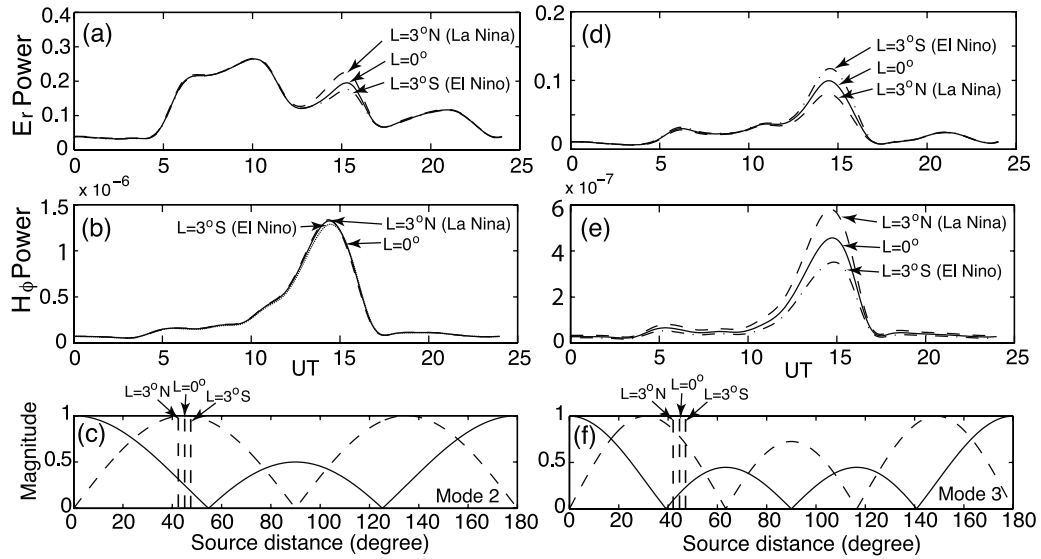


Figure 2. The diurnal power variations in the E_r and H_ϕ components of (a and b) the second and (d and e) third SR mode (L , the latitude of the lightning center in Africa). The spatial distribution functions of (c) the second and (f) third SR mode in the Earth-ionosphere cavity (solid lines, E_r component; dashed lines, H_ϕ component).

determined by $\sigma_e = N_e q_e \mu_e$, where q_e is the charge of the electron, N_e is the electron number density derived from International Reference Ionosphere (IRI) model [Bilitza, 2001], μ_e is the mobility of the electrons given by $\mu_e = 1.36 N_0 / N \frac{m^2}{Vs}$, where $N_0 = 2.688 \times 10^{25} m^{-3}$, and N is altitude dependent number density of air molecules [Pasko *et al.*, 1997]. The electron density in the cavity, N_e , is derived from the IRI model for a representative day of September 15, 2000 from 0000 UT to 2400 UT to account for the diurnal electron density variation. The total conductivity σ is derived as $\sigma = \sigma_i + \sigma_e$.

3. Results

[9] Figures 1b, 1c, 2a, 2b, 2d, and 2e report the FDTD results on the power variations in the E_r and H_ϕ components of the first three SR modes as a function of the universal time. The three curves in each figure describe the different power variation patterns associated with the different position of the lightning center in Africa during the El Niño, La Niña, and normal years. The African lightning center is located on the equator ($L = 0^\circ$) in the years without El Niño and La Niña. To account for the El Niño and La Niña, the African lightning center is shifted 3° southward ($L = 3^\circ S$) and northward ($L = 3^\circ N$), respectively. For the first mode, a significant power peak in both E_r and H_ϕ components related to the intensification of lightning activity in Africa is clearly observed around 1400 UT. The peak of E_r component decreases, but the peak of H_ϕ component increases when the lightning center shifts southward from $3^\circ N$ to $3^\circ S$. For the second mode shown in Figures 2a and 2b, the power peaks of the E_r component corresponding to the three centers of the lightning activity are found at 1000 UT, 1400 UT, and 2200 UT, respectively. The peak power of the E_r decreases with southward shift of African thunderstorm region from $3^\circ N$ to $3^\circ S$. However, no obvious power variation of the H_ϕ component at 1400 UT is observed in Figure 2b. For the third SR mode shown in Figures 2d

and 2e, the power of E_r and H_ϕ at 1400 UT increases and decreases with the southward moving of African lightning activity, respectively. Since we only change the position of the lightning activity in Africa in our FDTD simulations, only the obvious variations of the SR power near 1400 UT are clearly found, and the power peaks related to the lightning activity at South-East Asia and South America remain constant in these figures.

4. Discussion

[10] In our previous work [Yang and Pasko, 2006], we concluded that the SR power variation not only changes with the local and universal time, but also with the position of the receiver with respect to the lightning centers. The power peak appearing at 0500 UT in Figures 1b and 1c is related to the descent of the ionosphere due to the sunrise, and the second peak corresponds to the African lightning activity, which reaches the maximum at 1400 UT. Due to the nodal distance of the lightning centers in South-East Asia and South America with respect to the receiver, the lightning activity in these two regions contributes much less than that in Africa in Figures 1b and 1c.

[11] Although the distance between the simulated receivers in Hungary ($47.6^\circ N$, $16.7^\circ E$) and in Israel ($35.45^\circ E$, $30.35^\circ N$) [Price and Melnikov, 2004] is approximately 2500 km, for SR waves whose wavelength is comparable with the circumference of the Earth (40000 km), similar power variations are expected to be detected at these two observing stations. Comparing our FDTD results with the experimental measurements [Price and Melnikov, 2004, Figure 3], a similarity is found of the power variations of the E_r and H_ϕ components of the first three SR modes.

[12] The distributions of the E_r and H_ϕ components follow the Legendre ($P_n(\cos\theta)$) and associated Legendre ($P_n^1(\cos\theta)$) polynomials, where θ is the angular distance from the source to the receivers [e.g., Nikolaenko and Hayakawa, 2002, pp. 105]. Figures 1d, 2c and 2f show the

spatial distribution functions for the first three SR modes (E_r component is shown by solid line; H_ϕ component is shown by dashed line). The simulated lightning source is located at $\theta = 0^\circ$. For the SR station at Nagycenk, the angular distance between the station and the lightning on the equator in Africa is about 45° . Due to the northward and southward shifts of the lightning center, the angular distances are approximately 42° and 48° , respectively, in the La Niña and El Niño years. For the first SR mode, when the lightning center in Africa moves from 3°N to 3°S , the angular distance increases. In Figure 1d, the magnitude of the E_r and H_ϕ components monotonously increases and decreases, respectively, with the increase of the angular distance, providing straightforward explanation for why the power of the E_r and H_ϕ components undergoes opposite variation patterns shown in Figures 1b and 1c.

[13] For the second SR mode, since the magnitude of the E_r field monotonously decreases with increasing the angular distance (Figure 2c) around $\theta = 45^\circ$, a decrease of the E_r field magnitude around 1400 UT is obviously observed during the southward shift of the center of African lightning center (Figure 2a). There is a magnitude maximum of the H_ϕ component found at the position where $\theta = 45^\circ$ in Figure 2c, so the magnitude of H_ϕ almost remains constant around $\theta = 45^\circ$. Since the H_ϕ component is not sensitive to the shift of African lightning activity, we conclude that the second SR mode is not suitable to detect the motion of African lightning centers in this case.

[14] For the third SR mode, the E_r and H_ϕ power obviously increases and decreases with the southward shifts of African thunderstorm regions (shown in Figures 2d and 2e), respectively. All these features are in a good agreement with the specific electrical and magnetic field distributions shown in Figure 2f.

[15] Several techniques utilizing the modal distribution of SR electrical and magnetic components have been applied in past studies to locate the lightning activity [Polk, 1969; Jones and Kemp, 1970], and SR parameters (e.g., power and frequency) can be effectively employed to study the shifts of the thunderstorm regions related to El Niño and La Niña phenomena [Satori and Zieger, 1999; Nickolaenko and Hayakawa, 2002, pp. 264]. A power minima of E_r component for the first two modes in 1994 and other minima for the first mode in 1997/1998 due to a more southward position of the African thunderstorm region were reported by Satori and Zieger [1999]. A power maxima of the first SR mode was detected in the second half of 1996 and 1998 when African thunderstorm region shifts northward [Satori and Zieger, 1999]. All these features can be identified in our FDTD results shown in Figures 1b, 1c, 2a, and 2b.

[16] The intensity of the global lightning activity and the angular distance between the sources and receivers are two important factors to determine the magnitude of SR. The E_r and H_ϕ components both become stronger with the increase of the global lightning activity. However, the effects of the shift of the lightning centers on electrical and magnetic fields are different due to the different spatial field distributions of these components. For the first SR mode, the magnitude of the E_r component decreases with θ for $\theta < 90^\circ$, but increases for $\theta > 90^\circ$, and the H_ϕ component has an opposite variation tendency (shown in Figure 1d). There-

fore, in practice it is difficult to determine which factor (i.e., lightning intensity or angular distance) is the dominant reason to affect the SR power by considering only one field component (E_r or H_ϕ). For example, an increase of the magnitude of first SR E_r component may be equally well produced by the increasing lightning activity or by the shift of the lightning center closer to the receivers as $\theta < 90^\circ$. By using both electrical and magnetic components, the problem can be easily solved. The same power variation tendency of the E_r and H_ϕ components of the first SR mode would indicate that the variation of the intensity of lightning activity is the dominant factor to effect the SR power. The different power variations of the first SR mode electrical and magnetic components would show that the shift of the lightning center contributes more to the SR power variations, and the direction of the shift depends on the variation of both electrical and magnetic components and the angular distance between the lightning center and the receivers. For the SR stations which are located in Europe [e.g., Satori and Zieger, 1999; Price and Melnikov, 2004; Ondrášková et al., 2007], the angular distance to African thunderstorm center is within the range of $0^\circ < \theta < 90^\circ$. For the first SR mode, we predict that the intensity increase of the E_r component and the intensity decrease of the H_ϕ component would indicate that African thunderstorm center moves northward and therefore closer to these stations under La Niña conditions. The exactly opposite trend should be observed when the African thunderstorm center shifts southward under El Niño conditions. Using the same methodology, the SR data measured at the station located at Rhode Island (USA) [Williams and Satori, 2004] can be employed to remotely sense the thunderstorm activity in South America under El Niño and La Niña conditions.

[17] For the higher order modes shown in Figure 2, the field distributions are complicated, with the appearance of more maximum and null points. The field intensity does not change significantly with several degree variation of the source distance around these maximum or null points (e.g., Figure 2b). Therefore, the first SR mode is a better candidate for detecting the El Niño and La Niña effects than other modes. In the realistic SR measurements, the experimental data include all kind of external factors, such as diurnal and seasonal power variations, and the power variation associated with El Niño and La Niña phenomena. Since the time period of the El Niño and La Niña phenomena is much longer than the diurnal and seasonal cycles, the SR power variation associated with El Niño and La Niña phenomena can be clearly observed by averaging a long-term measurement data.

5. Conclusions

[18] The shift of the global lightning activity center associated with El Niño and La Niña phenomena is an important effect leading to the SR power variations. The effects of this shift on the SR power variations of the electrical and magnetic components are different from those produced by the intensity variation of the lightning activity. Due to the simplicity of the field distribution in the Earth-ionosphere cavity for the first SR mode, the combination of the electrical and magnetic components of the first SR mode is a good tool to detect the power variations of the lightning

activity and its spatial shift associated with the El Niño and La Niña phenomena. Same variation tendency of the first SR mode electrical and magnetic components indicates that the lightning activity dominates the SR power variation. The different variation tendency of the first SR mode electrical and magnetic components shows that the dominant effect leading to these power variations is the spatial shift of the thunderstorm regions. The direction of the shift depends on the spatial structure of the electrical and magnetic components and the angular distance between the thunderstorm region and the positions of the observing stations.

[19] **Acknowledgments.** This research was supported by NSF ATM-0134838 grant to Penn State University.

References

- Bilitza, D. (2001), IRI 2000, *Radio Sci.*, 36, 261.
- Hale, L. C. (1984), Middle atmosphere electrical structure, dynamics, and coupling, *Adv. Space Res.*, 4, 175.
- Hu, W., and S. A. Cummer (2006), An FDTD model for low and high altitude lightning-generated EM fields, *IEEE Trans. Antennas Propag.*, 54(5), 1513.
- Huang, E., E. Williams, R. Boldi, S. Heckman, W. Lyons, M. Taylor, T. Nelson, and C. Wong (1999), Criteria for sprites and elves based on Schumann resonance observation, *J. Geophys. Res.*, 104, 16,943.
- Jones, D. L., and D. T. Kemp (1970), Experimental and theoretical observations on the transient excitation of Schumann resonances, *J. Atmos. Terr. Phys.*, 32, 1095.
- Nickolaenko, A. P., and M. Hayakawa (2002), *Resonances in the Earth-Ionosphere Cavity*, Kluwer Acad., Norwell, Mass.
- Ondrášková, A., P. Kostecký, S. Ševčík, and L. Rosenberg (2007), Long-term observations of Schumann resonances at Modra Observatory, *Radio Sci.*, 42, RS2S09, doi:10.1029/2006RS003478.
- Otsuyama, T., D. Sakuma, and M. Hayakawa (2003), FDTD analysis of ELF wave propagation and Schumann resonances for a subionospheric waveguide model, *Radio Sci.*, 38(6), 1103, doi:10.1029/2002RS002752.
- Pasko, V. P., U. S. Inan, T. F. Bell, and Y. N. Taranenko (1997), Sprites produced by quasi-electrostatic heating and ionization in the lower ionosphere, *J. Geophys. Res.*, 102, 4529.
- Pasko, V. P., U. S. Inan, T. F. Bell, and S. C. Reising (1998), Mechanism of ELF radiation from sprites, *Geophys. Res. Lett.*, 25, 3493.
- Polk, C. (1969), Relation of ELF noise and Schumann resonances to thunderstorm activity, in *Planetary Electrodynamics*, vol. 2, edited by S. C. Coronoti and J. Hughes, p. 55, Gordon and Breach, New York.
- Price, C., and A. Melnikov (2004), Diurnal, seasonal, and inter-annual variations of the Schumann resonance parameters, *J. Atmos. Sol. Terr. Phys.*, 66, 1179.
- Sátori, G., and B. Zieger (1999), El Niño related meridional oscillation of global lightning activity, *Geophys. Res. Lett.*, 26, 1365.
- Schumann, W. O. (1952), Über die strahlungslosen einer leitenden Kugel die von einer Luftschicht und einer Ionosphärenhülle umgeben ist, *Z. Naturforsch. A.*, 7, 149.
- Sentman, D. D. (1995), Schumann resonances, in *Handbook of Atmospheric Electrodynamics*, pp. 267, CRC Press, London.
- Sentman, D. D., and B. J. Fraser (1991), Simultaneous observations of Schumann resonances in California and Australia: Evidence for intensity modulation by the local height of the D-region, *J. Geophys. Res.*, 96, 15,973.
- Simpson, J. J., and A. Taflove (2004), Two-dimensional FDTD model of antipodal ELF propagation and Schumann resonance of the Earth, *IEEE Trans. Antennas Propag.*, 52(2), 443.
- Taflove, A., and S. C. Hagness (2000), *Computational Electrodynamics: The Finite-Difference Time-Domain Method*, Artech House, Boston.
- Williams, E. R. (1992), The Schumann resonance—A global tropical thermometer, *Science*, 256(5060), 1184.
- Williams, E. R., and G. Sátori (2004), Lightning, thermodynamic, and hydrological comparison of the two tropical continental chimneys, *J. Atmos. Sol. Terr. Phys.*, 66, 1213.
- Yang, H., and V. P. Pasko (2005), Three-dimensional finite-difference time-domain modeling of the Earth-ionosphere cavity resonances, *Geophys. Res. Lett.*, 32, L03114, doi:10.1029/2004GL021343.
- Yang, H., and V. P. Pasko (2006), Three-dimensional finite-difference time-domain modeling of the diurnal and seasonal variations in Schumann resonance parameters, *Radio Sci.*, 41, RS2S14, doi:10.1029/2005RS003402.
- Yang, H., V. P. Pasko, and Y. Yair (2006), Three-dimensional finite-difference time-domain modeling of the Schumann resonance parameters on Titan, Venus, and Mars, *Radio Sci.*, 41, RS2S03, doi:10.1029/2005RS003431.

V. P. Pasko and H. Yang, Communications and Space Sciences Laboratory, Pennsylvania State University, 211B EE East, University Park, PA 16802, USA. (vpasko@psu.edu; hxy149@psu.edu)